J Comput Aided Mol Des (2006) 20:295–303
DOI 10.1007/s10822-006-9055-1

ORIGINAL PAPER

Pharmacophore model for bile acids recognition by the FPR receptor

Cristina Ferrari · Antonio Macchiarulo · Gabriele Costantino · Roberto Pellicciari

Received: 24 March 2006 / Accepted: 5 July 2006 / Published online: 14 September 2006

Abstract Formyl-peptide receptors (FPRs) belong to the family A of the G-protein coupled receptor superfamily and include three subtypes: FPR, FPR-like-1 and FPR-like-2. They have been involved in the control of many inflammatory processes promoting the recruitment and infiltration of leukocytes in regions of inflammation through the molecular recognition of chemotactic factors. A large number of structurally diverse chemotypes modulate the activity of FPRs. Newly identified antagonists include bile acids deoxycholic acid (DCA) and chenodeoxycholic acid (CDCA). The molecular recognition of these compounds at FPR receptor was computationally investigated using both ligand- and structure-based approaches. Our findings suggest that all antagonists bind at the first third of the seven helical bundles. A closer inspection of bile acid interaction reveals a number of unexploited anchor points in the binding site that may be used to aid the design of new potent and selective bile acids derivatives at FPR.

Keywords Antagonists · Bile acids · Formyl-peptide receptors · G-protein coupled receptors · Molecular modeling · Molecular recognition · Pharmacophore · Rational drug design

Abbreviations

GPCR	G protein-coupled receptor
FPR	formylpeptide receptor
FPRL-1	formyl peptide receptor like type-1
FPRL-2	formyl peptide receptor like type-2
DCA	deoxycholic acid
CDCA	chenodeoxycholic acid

C. Ferrari · A. Macchiarulo · G. Costantino · R. Pellicciari (✉)
Dipartimento di Chimica e Tecnologia del Farmaco, Università di Perugia, via del Liceo 1, 06127 Perugia, Italy
e-mail: rp@unipg.it

Introduction

Chemotactic factors are proteins produced at sites of inflammation or microbial infection [1–3] and, through signalling at specific G-protein coupled receptors (GPCRs), drive the accumulation of leukocites. In particular, chemotactic receptors comprise the members of the formyl peptide receptor class (FPRs) which includes three subtypes [4], termed formyl peptide receptor (FPR), formyl peptide receptor like type-1 (FPRL-1), defined as a low-affinity fMLF receptor, and type-2 (FPRL-2), which does not bind to N-formyl peptides. All the members of the FPRs class belong to the family A of the GPCR superfamily.

FPR is expressed on the membrane of neutrophils, monocytes, hepatocytes, immature dendritic cells, astrocytes, microglial cells and on the tunica media of coronary arteries. FPRL-1 is expressed on phagocytes, leukocytes, epithelial cells, T lymphocytes, neuroblastoma cells, astrocytoma cells and microvascular endothelial cells. FPRL-2 is expressed in monocytes but not in neutrophils. Formyl peptide receptors have been implicated in the control of many inflammatory processes promoting the recruitment and infiltration of neutrophils and phagocytes in districts of inflammation. For instance, FPRL-1 controls the pro-inflammatory responses observed in Alzheimer's disease (AD) [5] and prion diseases [6] promoting the infiltration of activated mononuclear phagocytes at sites of lesion.

Chemotactic factors that modulate FPRs comprise a small peptide produced by bacterial and mitochondrial proteins, termed the N-formyl-methionyl-leucyl-phenylalanine peptide (fMLF), and host-derived chemotactic agonists such as annexin-I [7], lipoxin-A4 (LXA4) [8], serum amyloid-A (SAA) [9] and a 42 amino-acid form of β amyloid peptide (Aβ42) [10].

However, a large number of structurally diverse chemotypes have been also identified to interact with FPRs. Among these, endogenous bile acids such as deoxycholic acid (DCA, **1**) and chenodeoxycholic acid (CDCA, **2**) are reported to antagonize FPRs at pathophysiological concentrations [11, 12]. This observation is particularly interesting since bile acids were considered for many years only as catabolic products of cholesterol, involved in lipid and vitamin solubilization and in the regulation of the enterohepatic circulation. In 1999 it was discovered that CDCA is the physiological ligand for a former orphan nuclear receptors, the Farneosid X Receptors (FXR) [13–15], thus unravelling an unexpected role for bile acids as signalling molecules. This role has been further substantiated by the recent discovery that bile acids are also agonists at the TGR5 receptor, a GPCR involved in regulating thyroid hormone signalling and energy homeostasis [16–18]. Taken together, these evidences support the notion that the bile acid scaffold owes structural features recognized by different targets. Thus, bile acid scaffold can be considered a ''privileged structure'' in the sense of being modulator of a broad spectrum of target families [19].

In the frame of a broader project aimed at clarifying the mechanism of bile acid recognition by receptor proteins [20, 21], we focus here on the task of gaining insights into the molecular basis of the interaction between bile acids and the formyl peptide receptors.

At this aim, a general pharmacophore model based on a large compilation of FPR antagonists is generated, focusing on the identification of those regions of bile acids responsible for FPR recognition. It should be mentioned that a pharmacophoric model of FPR antagonists has been recently reported [22] and its validity in retrieving active compounds using virtual screening of large chemical libraries has been demonstrated. However, our purpose was to investigate the molecular recognition of bile acid scaffold at FPR and the reported three point based pharmacophore of FPR did not cope with our aim.

Methods

All molecular modeling studies were carried out on a 2 CPU (PIV 2.0 GHz) linux machine.

For each compound molecular descriptors were calculated and were used as variables to perform a principal component analysis (PCA) with Molecular Operating Environment (MOE, version 2004.03) suite [23].

Pharmacophoric models and docking experiments were done with PHASE (version 1.0) and GLIDE (version 3.5) of Schrödinger's suite [24, 25].

PHASE automatically detects pharmacophoric features and generates annotations for each ligand. Then, it identifies common features among structurally diverse ligands through four steps: (1) a conformational search generates a set of conformers for each ligand using a continuum solvation treatment (MMFFs, GB/SA water). As the stereochemistry of Edward compounds are not known we let PHASE vary the chirality of atoms in the molecules; (2) pharmacophore sites are created from a set of features; (3) common pharmacophores are found using a tree-based partitioning technique that groups together similar features according to their intersite distances. In order to identify common pharmacophores PHASE samples the different steroisomers and locates the one that matches best; (4) The resulting pharmacophoric models are ranked according to the following scores: the *alignment score*, the *vector score* and a *volume score.*

The crystal structure of bovine rhodopsin (PDB code 1L9H) was used like template to build an homology model of FPR. The FPR and bovine rhodopsin sequences were aligned using MOEAlign. We constrained the alpha helixs, starting from the highly conserved residue as stated in the NIH GPCR database (http://mgddk1.niddk.nih.gov/GPCR.html), in order to avoid insertions/deletions in them. The loop was built by the loop search method implemented in MOE. Since the covalent link between cysteins in TM3 and E2 is conserved in the FPR receptor, the E2 loop was modeled using a rhodopsin-like constrained geometry around the disulfide bridge. We generated and refined the model with MOE using AMBER 94 force field. All antagonist structures were docked into FPR using GLIDE program. All variable parameters were set to the default values. The binding site was defined according to mutagenesis experiments. A rigid docking of both protein and molecules was performed using for each compound the bioactive conformation resulting from the pharmacophoric study.

Results and discussion

A collection of 32 compounds (Table 1) acting as potent or weak FPR antagonists were compiled from the literature. These include peptide derivatives of fMLF

Table 1 Compounds with FPR pIC50 or pKi data

ID	Structure	ID	Structure	ID	Structure
DCA (**1**) pIC50 = 4.00 I	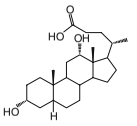	C119-0054 (**12**) pKi = 5.15 testset: II	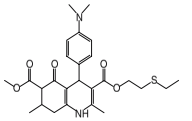	H2188-3197 (**23**) pKi = 5.00 testset: II	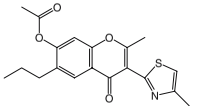
CDCA (**2**) pIC50 = 3.76 I	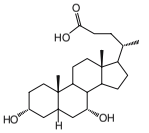	C142-0035 (**13**) pKi = 5.00 testset: II	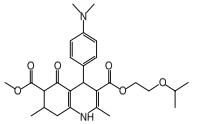	H2188-3754 (**24**) pKi = 5.22 testset: II	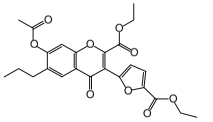
TBOC-FdLFdLF (**3**) pIC50 = 5.54 testset: I	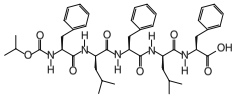	D4393-0018 (**14**) pKi = 4.92 testset: II	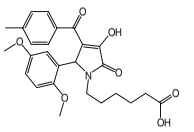	H3230-2889 (**25**) pKi = 5.00 testset: II	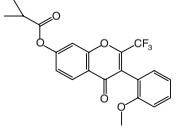
Isopropyl-ureido-FdLFdLF (**4**) pIC50 = 4.54 testset: I	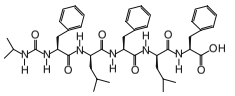	D4622-8438 (**15**) pKi = 4.92 testset: II	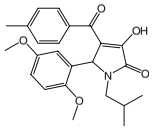	H3333-4944 (**26**) pKi = 4.92 testset: II	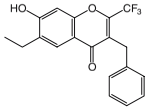
N-thiazolyl-ureido-FdLFdLF (**5**) pIC50 = 7.03 testset: I	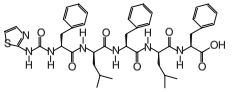	E1682-2106 (**16**) pKi = 5.40 testset: I	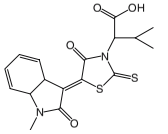	H3335-0327 (**27**) pKi = 5.70 testset: II	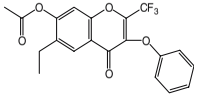
Sulfasalazine (**6**) pIC50 = 5.00 I	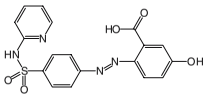	E1682-2108 (**17**) pKi = 5.22 testset: II	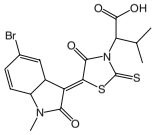	H3335-0384 (**28**) pKi = 4.66 testset: II	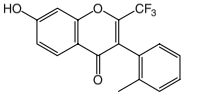
Losartan (**7**) I	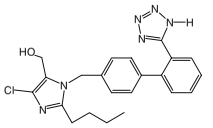	E3331-1295 (**18**) pKi = 5.15 testset: I	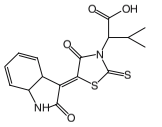	I2448-0030 (**29**) pKi = 4.80 testset: II	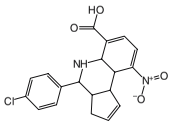

Table 1 Continued

ID	Structure	ID	Structure	ID	Structure
Phenylbutazone (**8**) pIC50 < 4.62 II	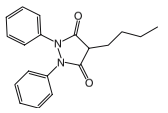	F6049-0473 (**19**) pKi = 5.10 testset: II	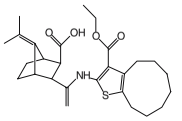	I3454-2064 (**30**) pKi = 4.92 testset: II	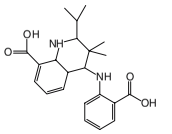
Sulphin-pyrazone (**9**) pIC50 = 4.62 II	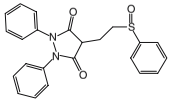	F6049-2423 (**20**) pKi = 4.96 testset: II	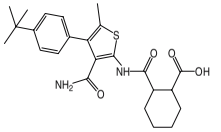	I4300-0286 (**31**) pKi = 4.59 testset: II	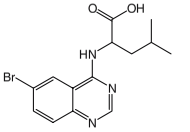
DPN (**10**) pIC50 < 4.62 II	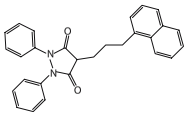	F6049-2563 (**21**) pKi = 4.55 testset: II	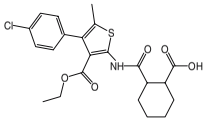	J4358-1479 (**32**) pKi = 4.68 testset: II	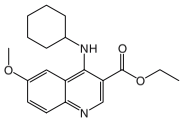
B6359-0291 (**11**) pKi = 5.40 testset: II	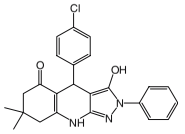	F6049-2738 (**22**) pKi = 4.68 testset: II	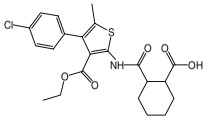		

obtained either by replacing the N-formyl group with a *tert*-butyloxy carbonyl (tBOC) (**3**) or *iso*-propylureido group (**4**) [26], or by peptide elongation and stereochemical inversion such as in the case of the potent N-ureido-Phe-D-Leu-Phe-D-Leu-Phe derivative (**5**) [27]; known anti-inflammatory and anti-hypertensive drugs such as Sulfasalazine (**6**) [28] and Losartan (**7**) [29]; CDCA (**2**) and deoxycholic acid (**1**) (DCA) that antagonize the activation of FPR at high but still physiological micromolar; phenylbutazone (**8**), sulfinpyrazone (**9**) and DPN (**10**) a diphenyl-3,5-pyrazolidinedione (3,5-P) derivatives [30]; 22 small molecule antagonists (**11–32**) identified in a high-throughput flow cytometry screening [22]. The structural diversity of the above set was assessed using a principal component analysis (PCA). In particular, the PCA was performed using constitutional molecular descriptors (number of acidic atoms, number of hydrophobic atoms, number of hydrogen bonding acceptors and donors) and physical property related descriptors (polar surface area, logP, molecular refractivity and total formal charge). The plot of the first two components, explaining respectively the 52.77% and 47.23% of the variance, is shown in Fig. 1.

Each dot represents a molecule encoded by its relative activity. The inspection of the plot reveals that molecules cluster into three groups. The first group contains bile acids and is located in the upper central region of the score plot. The Edwards derivates are found in the second group which is located in the lower portion of the plot. Peptides constitute the third group and are located in the lower right-hand region. Interestingly, the most active compounds do not occupy a specific region of the plot but are rather spread on the principal component space.

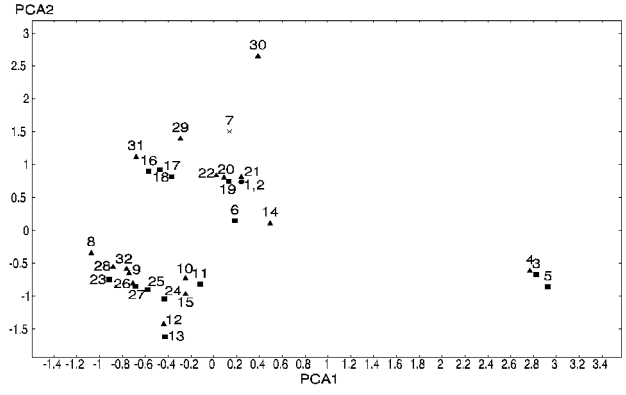

Fig. 1 Plot of the two first components. Compounds are displayed with different symbols according to three range of activity: ■ = pK_i–$pIC_{50} \geq 5$; ▲ = $4 < pK_i$–$pIC_{50} < 5$; • = pK_i–$pIC_{50} \leq 4$. As there is no activity data for losartan, this compound is represented with "×" symbol

In a first attempt, all molecules were used to construct a pharmacophoric model of FPR antagonists. We obtained a model based on three pharmacophoric points which included two hydrophobic centres and one hydrogen bonding acceptor site. In order to enrich the pharmacophore with additional features, we explored the hypothesis that not all the molecules in the set would have adopted the same binding pose into the receptor. This hypothesis is plausible given both the wide structural diversity of the set and the pharmacological profile of these molecules. Indeed, antagonists do not need to interact with the binding site using the same pose in order to achieve the block of the receptor.

Thus, we divided the original set into two dataset: a training set (10 compounds) and a test set (22 compounds). In particular, the training set was chosen in order to sample the entire PCA space. Peptide derivatives were arbitrarily kept out of the training set for their large number of torsional angles. This set was further subdivided into two groups according to the structural similarity of the molecules. The first active set comprised CDCA (**2**), DCA (**1**), losartan (**7**) and sulfasalazine (**6**). The second set comprised DPN (**10**), phenylbutazone (**8**) and sulphinpyrazone (**9**). We constructed a pharmacophoric model for each group of compounds. The first model (model I) is based on four anchor points: two hydrophobic centres (H_{I-2}, H_{I-3}), one hydrogen bonding donor site (D_{I-1}) and one hydrogen bonding acceptor/negative site (N/A_{I-4}) (Fig. 2). The pharmacophoric model of the second groups (model II) is endowed with five anchor points: two hydrogen bonding acceptor sites (A_{II-1}, A_{II-2}) and three hydrophobic centres (H_{II-3}, H_{II-4}, H_{II-5}) (Fig. 3).

The test set was fitted on both pharmacophoric models and they were classified in one of the two models according to their best fitness score. Five compounds (**3**, **4**, **5**, **16**, **18**), including small peptide derivatives, best fitted model I whereas the remaining compounds nicely matched the features of model II.

In particular, peptide derivatives (**3**, **4**, **5**) matched model I adopting a type II β-turn like conformation how depicted in Fig. 4.

Interestingly, the observed β-turn like conformations of peptides are in agreement with those reported by Dalpiaz et al. in circular dicroism and infrared absorption experiments for Phe-D-Leu-Phe-D-Leu-Phe derivatives [26]. In addition, it is known that these bioactive conformations occur in molecular events involving hormone-receptor and peptide-enzyme recognitions [31, 32]. An inspection of Fig. 3 reveals that both pharmacophoric models share some common features with similar distances of posing. Thus, we attempted a task to combine both pharmacophoric

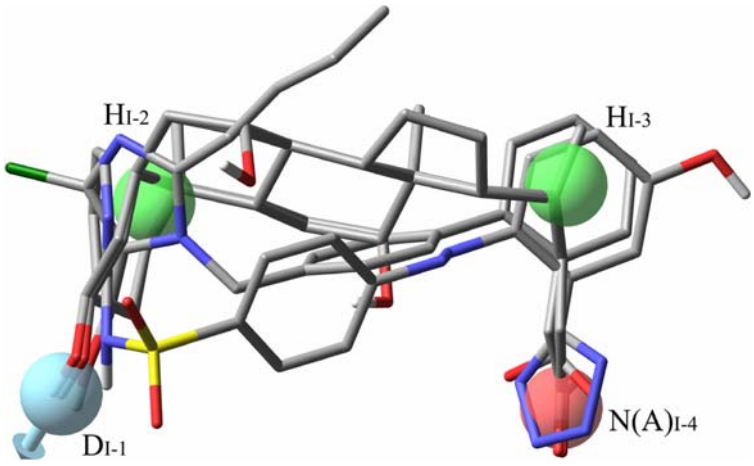

Fig. 2 Pharmacophoric model I

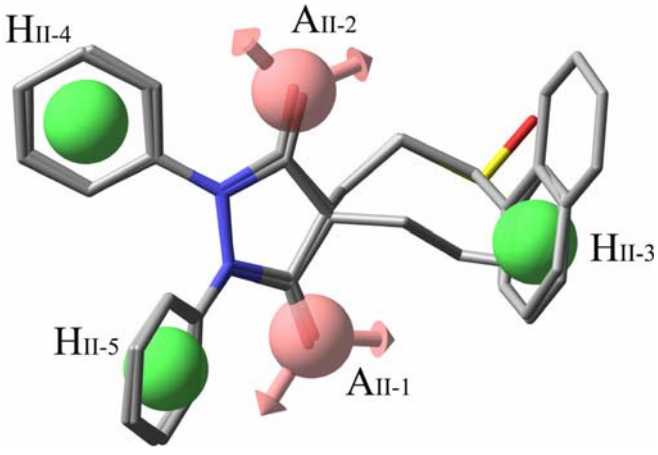

Fig. 3 Pharmacophoric model II

models. Thus, model I and model II were superimposed on the basis of their common features (Table 2).

During this procedure, we considered as common features also hydrogen bonding acceptor and donor sites. Indeed, this situation reflects the presence of aminoacidic side chains in the binding site that may both accept and donate hydrogen bonding (serine, threonine, tyrosine, glutamine and aspargine). Since all compounds are competitive modulators of FPR, one combination of both pharmacophoric models defines the entire binding pocket of the antagonists at the receptor. In order to identify the most likelihood combination, we constructed an homology model of the receptor based on the crystal structure of rhodopsin and performed docking experiments on models representing the possible pharmacophoric combinations.

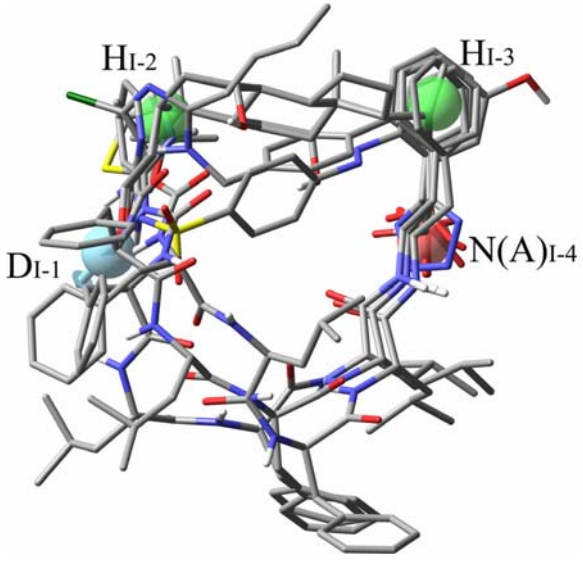

Fig. 4 Superposition of peptide antagonists onto model I

According to docking experiments, the best fitted combination of pharmacophoric models (pharmacophore model III) is the second top scored solution which shares a hydrogen bonding acceptor/donor site and a hydrophobic centre, how depicted in Fig. 5.

It is reported that the recognition of FPR agonists occurs in the upper region of the transmembrane (TM) helical bundle comprising TMs 2, 5, 6 and 7 [33]. In this region, ten residues affecting agonist binding have been identified by mutagenesis experiments [34]. These include Leu78 (TM2), Asp106 (TM3), Leu109 (TM3),

Table 2 Difference of the intersite distances in the pharmacophore models I and II

Pharmacophore model I intersite distance (Å)	Pharmacophore II intersite distance (Å)	Delta Intersite distances (Å)
N(A)4-H3 = 4.381	A2-H3 = 5.351	Δ = 0.97
N(A)4-H3 = 4.381	A1-H3 = 4.616	Δ = 0.235
D1-H2 = 4.3	A2-H3 = 5.351	Δ = 1.051
D1-H2 = 4.3	A1-H3 = 4.616	Δ = 0.316
D1-H2 = 4.3	A2-H2 = 4.622	Δ = 0.322
D1-H2 = 4.3	A1-H5 = 4.033	Δ = 0.267

of antagonists. Very recently, indeed, extracellular loops of GPCRs have been indicated as containing recognition sites for peptide ligands [35]. Therefore, we gave particular attention to the second extracellular loop (E2), which has been described to fold back over TM helices, limiting the size of the active site [36]. In particular, some residues of E2 could be involved in antagonist binding. The construction and the exploration of the conformational profile of loop E2 was carried out as discussed in the method section. The

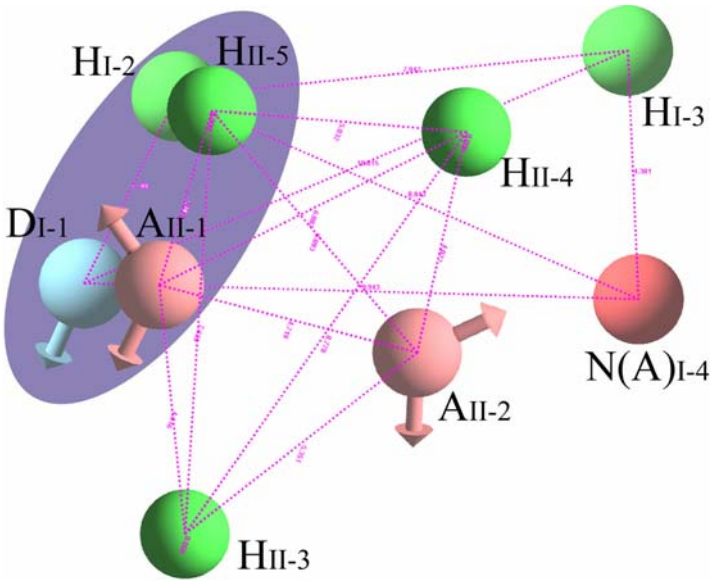

Fig. 5 Pharmacophoric sites superimposed according to the lower difference in inter-site distances

Thr157 (TM4), Arg201 (TM5), Ile204 (TM5), Arg205 (TM5), Trp254 (TM6), Tyr257 (TM6) and Phe291 (TM7).

Docking results suggest that the binding site of antagonists is slightly different in respect to that of agonists. Indeed residues D106, R201 and R205, which were showed to be important in determining the anchoring at the receptor of the formyl moiety (D106 and R201) and the carboxyl terminal group of fMLF, seem to be not involved in the binding of the antagonists considered in this study. These compounds bind to a site located at the outer side of the TM helices, between loops E2 and E3. It should be mentioned, however, that docking experiments suffer the limitation related to the flexible conformational profile of side chain of residues delineating the TM helices that is hardly predictable. Thus, it cannot be ruled out that the combined pharmacophoric model of antagonists may fit the 3D model of FPR in alternative solutions which involve the above residues. Nevertheless, we thought to take into account the obtained docked solution and to explore the role of extracellular loops in recognition inspection of the obtained fit of the combined pharmacophoric model into FPR model comprising loop E2 reveals that antagonists block the access of agonists to the receptor (Fig. 6a).

In the docked pose, the hydrogen bonding site ($D_{I\text{-}1}$, $A_{II\text{-}2}$) is placed close to Thr265 (TM6) while the hydrophobic ($H_{I\text{-}2}$, $H_{II\text{-}5}$) constitutes the centre of an hydrophobic cluster comprising Pro168 (E2), Phe180 (E2) and Leu272 (E3). The hydrogen bonding acceptor site of Model I ($N/A_{I\text{-}4}$) matches Tyr257 (TM6) whereas its second hydrophobic point ($H_{I\text{-}3}$) is projected toward Ala (175), the carbon chain of Lys170 (E2) and Phe291 (TM7). One of the remaining hydrophobic points of Model II ($H_{II\text{-}3}$) is located near residues Val200 (TM5), Phe206 (TM5), Val160 (TM4) and Phe102 (TM3). The second hydrophobic point ($H_{II\text{-}4}$) is docked within a hydrophobic pocket constituted by residue of TM6 (Val260, Ala261, Tyr257) and TM7 (Val283). The last hydrogen bonding acceptor site of Model II ($A_{II\text{-}1}$) seems not making specific interactions with the conformation of the receptor used for docking experiments.

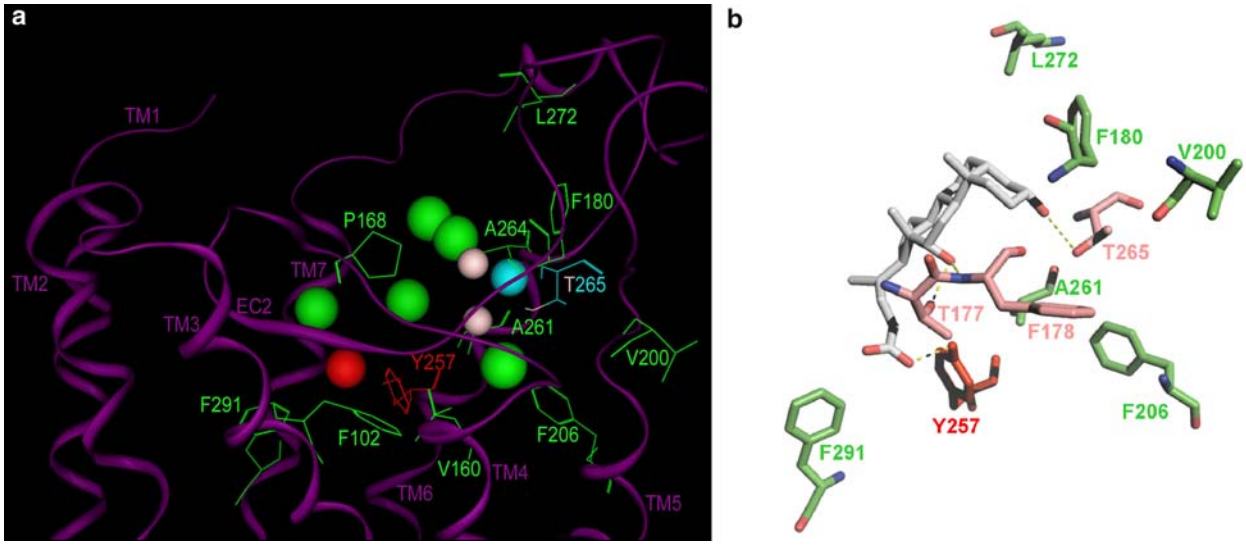

Fig. 6 (**a**) Docking of the superimposed pharmacophoric model into the binding site of FPR. Non polar hydrogen atoms are not displayed. Aminoacids are colored according to the colors of the matching pharmacophoric feature. (**b**) Analysis of the binding mode of DCA in which the interaction with the most crucial amino acids are highlighted

A closer inspection of bile acids binding at FPR receptor reveals that steric and electrostatic complementarities exist between DCA (**1**) and the receptor (Fig. 6b). In the docked pose, the steroid nucleus of (**1**) is oriented parallel to the plane of the lipid bilayer, with the carboxylic moiety and the ring A in proximity respectively to TM6 and TM7, and to TM5 and TM6. Three stabilizing hydrogen-bonding interactions are observed between DCA (**1**) and Thr265 (TM6), Thr177 (E2), Tyr257 (TM6). While the interaction with Tyr257 is crucial for anchoring the carboxylic moiety of bile acids to the receptor, hydrogen bonding with Thr177 and Thr265 is important to determine the potency of bile acids. Indeed, the potency of DCA (**1**) accounts for the additional hydrogen bonding observed between the 12α hydroxyl group and Thr177. The 12α hydroxyl group is lacking in CDCA (**2**). Thus, only the hydrogen bonding between the 7α hydroxyl group and Thr265 is present. In order to gain insight into the appropriate decorations of bile acids scaffold required to improve the potency, we plotted the combined pharmacophoric model around the nucleus of DCA (**1**).

In particular, considering DCA (**1**) as lead compound, two positions are interesting for chemical modifications: 3α and 15. The 3α position could be decorated with alkyl-ether groups in order to accept an hydrogen bond from Thr265 (TM6) and occupy a pocket of FPR yielding hydrophobic interactions with Val200 (TM5), Phe206 (TM5), Val160 (TM4) and Phe102 (TM3). According to the combined pharmacophore (model III), these derivates would fit the hydrophobic feature defined by groups in position 4 of 3,5-pyrazolidinediones. In addition, small alkyl groups can be placed in position 15 in order to make hydrophobic interactions with Val283 (TM7), Ala 261 and Ala 264 (TM6). These groups would fit the hydrophobic feature $H_{II\text{-}4}$ of the combined pharmacophore.

Conclusions

Bile acids are endogenous metabolites which are known to be involved in the control of dietary lipid absorption and cholesterol catabolism through the activation of nuclear receptors. Very recently, a number of experimental evidences point out important roles for bile acids as signalling molecules acting at G-protein coupled receptors. Hence, the development of potent and selective bile acids derivatives is a challenging task which enables the availability of chemical tools to disclose novel physiological functions of bile acids and related receptors across different therapeutic areas. In this work, we pursue the concept of bile acids as privileged structures to design new modulators of formyl peptide receptor (FPR). Thus, we developed a combined ligand- and structure-based approach to describe the binding mode of known FPR antagonists and bile acids at the receptor. In the resulting binding mode, all compounds block the access of agonists to the receptor and may interfere with conformational movements of extracellular loops linked to receptor activation [35]. A closer inspection of DCA (**1**) binding at FPR receptor reveals three hydrogenbonding interactions. The hydrogen bonding interaction with Tyr257

is crucial for anchoring the carboxylic moiety of bile acids. The presence/absence of the remaining two hydrogen bonding interactions accounts for the potency of DCA (**1**) over CDCA (**2**). Several other interaction features emerge from the inspection of the binding mode of the remaining FPR antagonists. Overall, these results will be useful to guide the selection of the appropriate chemical decorations of steroid scaffold in order to design potent and selective bile acids derivatives at formyl peptide receptors.

References

1. Marasco WA, Phan SH, Krutzsch H, Showell HJ, Feltner DE, Nairn R, Becker EL, Ward PA (1984) J Biol Chem 259:5430
2. Schiffmann E, Showell HV, Corcoran BA, Ward PA, Smith E, Becker EL (1975) J Immunol 114:1831
3. Carp H (1982) J Exp Med 155:264
4. Le Y, Murphy PM, Wang JM (2002) Trends Immunol 23:541
5. Iribarren P, Zhou Y, Hu J, Le Y, Wang JM (2005) Immunol Res 31:165
6. Le Y, Yazawa H, Gong W, Yu Z, Ferrans VJ, Murphy PM, Wang JM (2001) J Immunol 166:1448
7. Walther A, Riehemann K, Gerke V (2000) Mol Cell 5:831
8. Takano T, Fiore S, Maddox JF, Brady HR, Petasis NA, Serhan CN (1997) J Exp Med 185:1693
9. Su SB, Gong W, Gao JL, Shen W, Murphy PM, Oppenheim JJ, Wang JM (1999) J Exp Med 189:395
10. Le Y, Gong W, Tiffany HL, Tumanov A, Nedospasov S, Shen W, Dunlop NM, Gao JL, Murphy PM, Oppenheim JJ, Wang JM (2001) J Neurosci 21:RC123:1
11. Chen X, Mellon RD, Yang L, Dong H, Oppenheim JJ, Howard OM (2002) Biochem Pharmacol 63:533
12. Chen X, Yang D, Shen W, Dong HF, Wang JM, Oppenheim JJ, Howard MZ (2000) Inflamm Res 49:744
13. Wang H, Chen J, Hollister K, Sowers LC, Forman BM (1999) Mol Cell 3:543
14. Parks DJ, Blanchard SG, Bledsoe RK, Chandra G, Consler TG, Kliewer SA, Stimmel JB, Willson TM, Zavacki AM, Moore DD, Lehmann JM (1999) Science 284:1365
15. Makishima M, Okamoto AY, Repa JJ, Tu H, Learned RM, Luk A, Hull MV, Lustig KD, Mangelsdorf DJ, Shan B (1999) Science 284:1362
16. Maruyama T, Miyamoto Y, Nakamura T, Tamai Y, Okada H, Sugiyama E, Nakamura T, Itadani H, Tanaka K (2002) Biochem Biophys Res Commun 298:714
17. Kawamata Y, Fujii R, Hosoya M, Harada M, Yoshida H, Miwa M, Fukusumi S, Habata Y, Itoh T, Shintani Y, Hinuma S, Fujisawa Y, Fujino M (2003) J Biol Chem 278:9435
18. Watanabe M, Houten SM, Mataki C, Christoffolete MA, Kim BW, Sato H, Messaddeq N, Harney JW, Ezaki O, Kodama T, Schoonjans K, Bianco AC, Auwerx J (2006) Nature 439:484
19. Muller G (2003) Drug Discov Today 8:681
20. Costantino G, Macchiarulo A, Entrena-Guadix A, Camaioni E, Pellicciari R (2003) Bioorg Med Chem Lett 13:1865
21. Costantino G, Entrena-Guadix A, Macchiarulo A, Gioiello A, Pellicciari R (2005) J Med Chem 48:3251
22. Edwards BS, Bologa C, Young SM, Balakin KV, Prossnitz ER, Savchuck NP, Sklar LA, Oprea TI (2005) Mol Pharmacol 68:1301
23. C.C.G. Inc (2005) Molecular operating Environment (MOE)
24. Schroedinger LLC New York, GLIDE 3.5 (2005)
25. Schroedinger LLC New York, PHASE 1.0 (2005)
26. Dalpiaz A, Ferretti ME, Pecoraro R, Fabbri E, Traniello S, Scatturin A, Spisani S (1999) Biochim Biophys Acta 1432:27
27. Dalpiaz A, Ferretti ME, Vertuani G, Traniello S, Scatturin A, Spisani S (2002) Eur J Pharmacol 436:187
28. Stenson WF, Mehta J, Spilberg I (1984) Biochem Pharmacol 33:407
29. Raiden S, Giordano M, Andonegui G, Trevani AS, Lopez DH, Nahmod V, Geffner JR (1997) J Pharmacol Exp Ther 281:624
30. Levesque L, Gaudreault RC, Marceau F (1991) Can J Physiol Pharmacol 69:419
31. Kitagawa O, Van der Velde D, Dutta D, Morton M, Takusagawa F, Aubé J (1995) J Am Chem Soc 19:5169
32. Tran TT, McKie J, Meutermans WD, Bourne GT, Andrews PR, Smythe ML (2005) J Comput Aided Mol Des 19:551
33. Miettinen HM, Mills JS, Gripentrog JM, Dratz EA, Granger BL, Jesaitis AJ (1997) J Immunol 159:4045
34. Mills JS, Miettinen HM, Cummings D, Jesaitis AJ (2000) J Biol Chem 275:39012
35. Klco JM, Nikiforovich GV, Baranski TJ (2006) J Biol Chem 281:12010
36. Perez HD, Vilander L, Andrews WH, Holmes R (1994) J Biol Chem 269:22485